Available online at www.sciencedirect.com
ScienceDirect
Biochimica et Biophysica Acta 1777 (2008) 351–361
Biochimica et Biophysica Acta BBA
www.elsevier.com/locate/bbabio

Photosystem I complexes associated with fucoxanthin-chlorophyll-binding proteins from a marine centric diatom, *Chaetoceros gracilis*

Yohei Ikeda [a], Masayuki Komura [b], Mai Watanabe [a], Chie Minami [a], Hiroyuki Koike [a], Shigeru Itoh [b], Yasuhiro Kashino [a,*], Kazuhiko Satoh [a]

[a] *Graduate School of Life Science, University of Hyogo, Harima Science Garden City, Hyogo 678-1297, Japan*
[b] *Graduate School of Science, Nagoya University, Furo-cho, Chikusa, Nagoya 464-8601, Japan*

Received 19 September 2007; received in revised form 30 January 2008; accepted 30 January 2008
Available online 12 February 2008

Abstract

Diatoms occupy a key position as a primary producer in the global aquatic ecosystem. We developed methods to isolate highly intact thylakoid membranes and the photosystem I (PS I) complex from a marine centric diatom, *Chaetoceros gracilis*. The PS I reaction center (RC) was purified as a super complex with light-harvesting fucoxanthin-chlorophyll (Chl)-binding proteins (FCP). The super complex contained 224 Chl *a*, 22 Chl *c*, and 55 fucoxanthin molecules per RC. The apparent molecular mass of the purified FCP–PS I super complex (~1000 kDa) indicated that the super complex was composed of a monomer of the PS I RC complex and about 25 copies of FCP. The complex contained menaquinone-4 as the secondary electron acceptor A_1 instead of phylloquinone. Time-resolved fluorescence emission spectra at 77 K indicated that fast (16 ps) energy transfer from a Chl *a* band at 685 nm on FCP to Chls on the PS I RC complex occurs. The ratio of fucoxanthin to Chl *a* on the PS I-bound FCP was lower than that of weakly bound FCP, suggesting that PS I-bound FCP specifically functions as the mediator of energy transfer between weakly bound FCPs and the PS I RC.

Keywords: *Chaetoceros gracilis*; Diatom; Fucoxanthin-chlorophyll-binding protein; Photosystem I; Time-resolved fluorescence spectra

1. Introduction

Diatoms contribute to the global carbon cycle and hence to the regulation of the global climate [1] by performing around 40% of the photosynthetic carbon fixation in the oceans [2], which accounts for ~20% of the global annual primary production [3]. Thus diatoms are an important focus of scientific research (e.g., [4]). Exemplifying their importance, the DNA sequences of the complete nuclear and chloroplast genomes are now available for a centric diatom, *Thalassiosira pseudonana*, and a pennate diatom, *Phaeodactylum tricornutum* [5,6] (http://genome.jgi-psf.org/Phatr2/Phatr2.home.html).

The physico-chemical environments of phytoplankton fluctuate frequently in the ocean [7]. Diatoms have been assumed to acclimatize to environmental changes by a mechanism somewhat different from that of higher plants [8]. Reduction of light intensity decreases the ratio of photosystem (PS) II to PS I in cyanobacteria, green algae and vascular plants, whereas in a pennate diatom, *Cylindrotheca fusiformis*, the ratio increased from 1.3 to 3.9 [9]. A similar result was reported for a marine centric diatom, *Skeletonema costatum* [10], although contrasting results are also reported [4]. The PS II:PS I ratios reported for diatoms exceed 1.0 and are larger than those of cyanobacteria (~0.1) and higher plants (~1.0) [8,11].

In most photosynthetic organisms the number of antenna pigment–protein complexes changes in response to environmental

Abbreviations: BN-PAGE, blue-native polyacrylamide gel electrophoresis; 2,5-DCBQ, 2,5-dichloro-*p*-benzoquinone; DD, diadinoxanthin; DDM, *n*-dodecyl-β-D-maltopyranoside; DT, diatoxanthin; Chl, chlorophyll; FCP, fucoxanthin-chlorophyll-binding protein; HPLC, high performance liquid chromatography; LHC, light-harvesting chlorophyll protein; MES, 2-morpholinoethanesulfonic acid; MK-4, menaquinone-4; PhQ, phylloquinone; PS I and PS II, photosystems I and II; RC, reaction center; SDS-PAGE, sodium dodecyl sulfate-polyacrylamide gel electrophoresis; Tc, time constant; TRFS, time-resolved fluorescence spectra; Vx, violaxanthin

* Corresponding author. Department of Life Science, University of Hyogo, 3-2-1 Kohto, Kamigohri, Ako-gun, Hyogo 678-1297, Japan. Tel./fax: +81 791 58 0185.
E-mail address: kashino@sci.u-hyogo.ac.jp (Y. Kashino).

0005-2728/$ - see front matter © 2008 Elsevier B.V. All rights reserved.
doi:10.1016/j.bbabio.2008.01.011

changes in light intensity, as typically occurs with chlorophyll (Chl) *a/b* protein in green plants and green algae [8,12]. However, in diatoms the ratio of accessory pigments to Chl *a* does not change significantly [9,10,12,13]. This seems to be related to diatoms' specific light-harvesting antenna complex with unique accessory pigments; Chl *c*, fucoxanthin, diadinoxanthin (DD) and diatoxanthin (DT) are components of the fucoxanthin-Chl binding proteins (FCP) [14]. DD and DT are the representative pigments of a unique xanthophyll cycle that protects their photosystems under high irradiance [15–18].

Biochemical studies of diatom photosynthetic systems are rare [5,19] because of the difficulty of isolating photoactive thylakoid membranes from the cells, which have hard silicate shells. Thylakoid membranes isolated from *C. fusiformis* after disruption with a French pressure cell exhibited a rate of oxygen evolution about half of that in the intact cells [20]. Berkaloff et al. isolated a P700 (a reaction center (RC) Chl dimer of PS I)-enriched fraction from *P. tricornutum* with digitonin [19]. Further solubilization of the P700-enriched fraction with *n*-dodecyl-β-D-maltopyranoside (DDM) released polypeptides of around 20 kDa, which were assumed to be a light-harvesting Chl protein (LHC) associated with the PS I complex. Recently, Brakemann et al. isolated thylakoid membranes from a centric diatom, *Cyclotella cryptica*, using a French pressure cell [21]. Pigment-containing fractions obtained by sucrose density gradient centrifugation or deriphate-polyacrylamide gel electrophoresis after solubilization of the thylakoid membranes with 10% DDM were shown to be PS I and PS II complexes associated with FCP [21]. The composition of the PS I complex of diatoms, however, has not been precisely determined yet.

In this study we report new methods for isolating highly photoactive thylakoid membranes and the PS I complex from a marine centric diatom, *Chaetoceros gracilis*. The purified PS I complex contained tightly-bound FCPs that transfer excitation energy to PS I. Blue native polyacrylamide gel electrophoresis (BN-PAGE) and size-exclusion chromatography revealed the PS I complex to be a monomer with antenna FCPs similar to the pea PS I with Chl *a/b* LHC [22], rather than a trimer as in the PS I of cyanobacteria [23].

2. Materials and methods

2.1. Culture conditions

The centric diatom, *C. gracilis* Schütt (UTEX LB2658), was grown photoautotrophically in 7.5 L F/2 medium [24] supplemented with artificial sea water (Sigma, St. Louis, MO), which was aerated with air containing 5% CO_2, at 20 °C for 6–8 d in a 9 L polycarbonate square bottle (Nalge Nunc, Rochester, NY). Continuous light was supplied by two 22 W fluorescent bulbs (Toshiba, Tokyo, Japan) placed on the opposite sides of the bottle. The light intensity at the surface facing the light source was 13 μmol photons m^{-2} s^{-1}. Cells in a late logarithmic-phase were collected by centrifugation (3000×*g*, 15 min) and resuspended in buffer A (50 mM 2-morpholinoethanesulfonic acid (MES)-NaOH (pH 6.0), 10 mM $MgCl_2$, 5 mM $CaCl_2$) supplemented with 25% glycerol (buffer B). The collected cells were frozen and stored at −80 °C until use.

2.2. Purification of PS I complexes from Chaetoceros gracilis

All procedures were performed under room or dim light at 4 °C. After addition of DNase I (~0.5 μg mL^{-1}) (Sigma) and protease inhibitor cocktail (250 μL/100 mL cell suspension) (Sigma) to the thawed cell suspension, thylakoid membranes were precipitated by centrifugation (40,000×*g*, 15 min) and washed once in buffer A. The thylakoid membranes were resuspended in buffer A supplemented with 1 M betaine at 1 mg Chl *a* mL^{-1} and solubilized with 0.5–1.0% w/v *n*-dodecyl-β-D-maltopyranoside (DDM) (Anatrace, Maumee, OH) for 10 min on ice. The suitable concentrations of DDM were determined in prior preliminary experiments for each of the cultures so that solubilized thylakoid membranes accounted for 60–70% of Chl *a* (w/w). The solubilized thylakoid membranes obtained after centrifugation (6000×*g*, 15 min) were loaded on a stepwise sucrose density gradient comprising 6 mL solutions of 0.4 M, 0.6 M and 0.8 M sucrose in buffer A supplemented with 0.04% DDM. After centrifugation (300,000 ×*g*, 2 h) the pellet was resuspended in buffer B containing 0.04% DDM. After removal of unsolubilized materials by centrifugation (9000 ×*g*, 15 min), the PS I-enriched supernatant was applied to size-exclusion chromatographs (HiPrep 16/60 Sephacryl S-300 HR, GE Healthcare UK Ltd., Buckinghamshire, England) with buffer B containing 0.04% DDM at a flow rate of 0.5 mL min^{-1}. The elution was monitored at 280 nm. Molecular mass was estimated using a PS I trimer from *Synechocystis* sp. PCC 6803 (~1000 kDa) obtained as a flow-through fraction at a purifying step for PS II complexes [25], ferritin (440 kDa), catalase (232 kDa) and aldolase (158 kDa) as molecular-mass markers. The peak fraction accounting for only 1% Chl *a* (w/w) in the thylakoid membrane preparation was collected and the PS I complexes were precipitated by centrifugation (40,000 ×*g*, 15 min) in the presence of 15% polyethylenglycol 8000 and resuspended in buffer B containing 0.04% DDM.

2.3. Isolation of PS I-enriched membranes from spinach

PS I-enriched membranes were prepared as a Triton X100-solubilized stromal thylakoid fraction from spinach purchased at a local market [26].

2.4. Polypeptide analysis

Sodium dodecyl sulfate-polyacrylamide gel electrophoresis (SDS-PAGE) and N-terminal amino acid sequencing using a protein sequencer PSQ-1 (Shimadzu, Kyoto, Japan) were performed as described in [27]. PsaA/PsaB and FCPs were identified immunologically using specific antibodies against PsaA/B [28] and FCPs from the raphidophyte *Heterosigma akashiwo* (obtained from Prof. B. R. Green of the University of British Columbia). For immunodetection, bands were visualized using enhanced chemiluminescence reagents (WestPico; Pierce) on a Fujifilm LAS-1000 imager (Fujifilm, Tokyo, Japan). BN-PAGE was performed as described in [29] with a 2.5–13% T acrylamide separation gel and 2.5% T acrylamide stacking gel run at 4 °C using PS I complexes equivalent to 6 μg Chl *a*. Molecular mass of the PS 1 complexes was estimated using the set of standard proteins for size-exclusion chromatography, as described in section 2.2, supplemented with thyroglobulin (669 kDa). Second-dimensional SDS-PAGE was conducted using a Tris/MES gel system with a 18–24% gradient acrylamide gel containing 6 M urea as described in [27].

2.5. Analysis of pigments and quinones

The amounts of menaquinone-4 (MK-4), phylloquinone (PhQ), and photosynthetic pigments were determined by reverse-phase high performance liquid chromatography (HPLC) with a Prodigy 5 (ODS 3, 100 Å) column (150×4.60 mm) (Phenomenex Inc., Torrance, CA) and a Shimadzu LC-10 AD system with a SCL-10A controller using a gradient of solvents as described previously [18]. Pigments and quinones were extracted using *N*,*N*-dimethylformamide [30] prior to HPLC analysis. Pigment extracts equivalent to 0.25–0.6 μg Chl *a* were injected. Pigment absorption patterns were detected with a Shimadzu SPD-M10AVP photodiode array detector and analyzed with Shimadzu CLASS-M10A software. MK-4 and PhQ quantities were determined at 270 nm and the amount of photosynthetic pigments was determined at 430 nm. MK-4 and PhQ levels were calibrated using extinction coefficients described in [31]. The amount of photochemically active P700 was assessed by the reduction in light-induced absorbance at 700 nm using a MPS2000 UV–VIS spectrophotometer (Shimadzu) at room temperature with 10 μg Chl *a* mL^{-1}. The reaction mixture contained 1 mM methylviologen as an electron acceptor, and 0.5 mM sodium ascorbate and 10 μM 2,6-dichlorophenolindophenol as electron donors in buffer

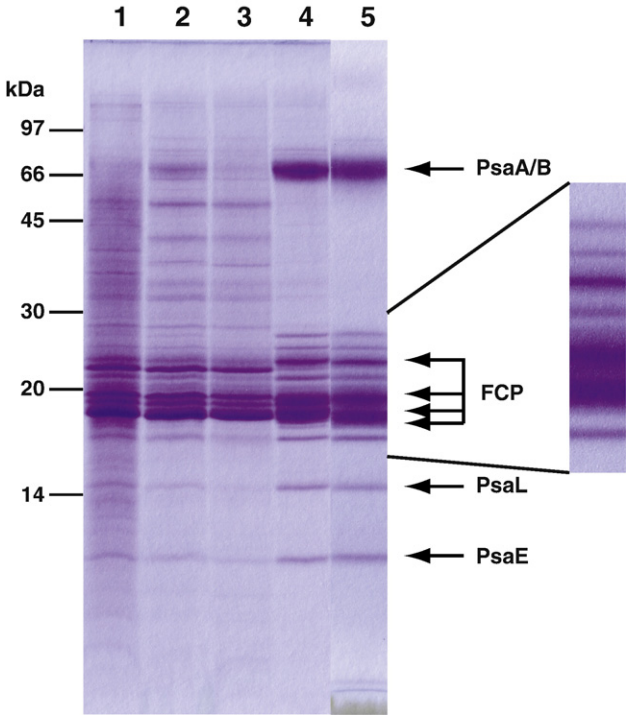

Fig. 1. Polypeptide profiles of preparations at different stages of PS I complex purification from *Chaetoceros gracilis*. Lane 1, thylakoid membranes; 2, solubilized thylakoid membranes; 3, FCP fraction; 4, PS I-enriched fraction after centrifugation; 5, purified FCP–PS I super complexes. Proteins equivalent to 10 μg Chl *a* were applied to each lane and were stained by Coomassie Blue. Arrows indicate the proteins that were identified in this study. The positions of molecular-mass standards are shown on the left. The central part of lane 5 is magnified to show FCP bands more clearly.

B containing 0.04% DDM. P700 content was calculated using a reduced minus oxidized extinction coefficient of 70 mM^{-1} cm^{-1} [32]. Chl concentration was determined using the method described in [33] for diatom samples and the method described in [34] for spinach samples.

2.6. Oxygen-evolving activity

The rate of oxygen evolution was assessed using a Clark-type oxygen electrode with 0.5 mM 2,5-dichloro-*p*-benzoquinone (DCBQ) as an electron acceptor at 30 °C with 10 μg Chl *a* mL^{-1}. Buffer B and F/2 culture medium were used as reaction mixtures for isolated thylakoid membranes and intact cells, respectively.

2.7. Absorption and fluorescence spectroscopy

Absorption spectra at room temperature were measured using either a UVIKON 922 spectrophotometer (Kontron Instruments, Milan, Italy) or MPS2000 UV–VIS spectrophotometer with 5 μg Chl *a* mL^{-1}. Absorption

Table 1
The rate of oxygen evolution in intact cells and isolated thylakoid membranes from *Chaetoceros gracilis*

	Rate of oxygen evolution ($\mu mol\ O_2\ mg^{-1}$ Chl *a* 1)
Intact cells	230±3.5
Thylakoid membranes	230±12

The activity was measured using 0.5 mM 2,5-DCBQ as an electron acceptor at 30 °C at 10 μg Chl *a* mL^{-1} (n=3).

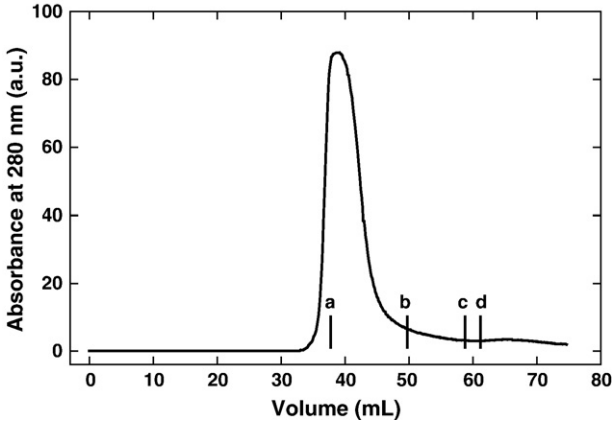

Fig. 2. Elution pattern of PS I complexes of *Chaetoceros gracilis* from size-exclusion column chromatography. The peak positions of molecular-mass markers are shown by vertical bars; (a) PS I trimer from *Synechocystis* 6803 (~1000 kDa), (b) ferritin (440 kDa), (c) catalase (232 kDa) and (d) aldolase (158 kDa).

spectra at 5 K were measured following [35] after addition of the same volume of glycerol as a cryoprotectant. Steady-state fluorescence emission spectra at 77 K were measured using a H-20 UV monochromator (Jobin Yvon, Cedex, France) as

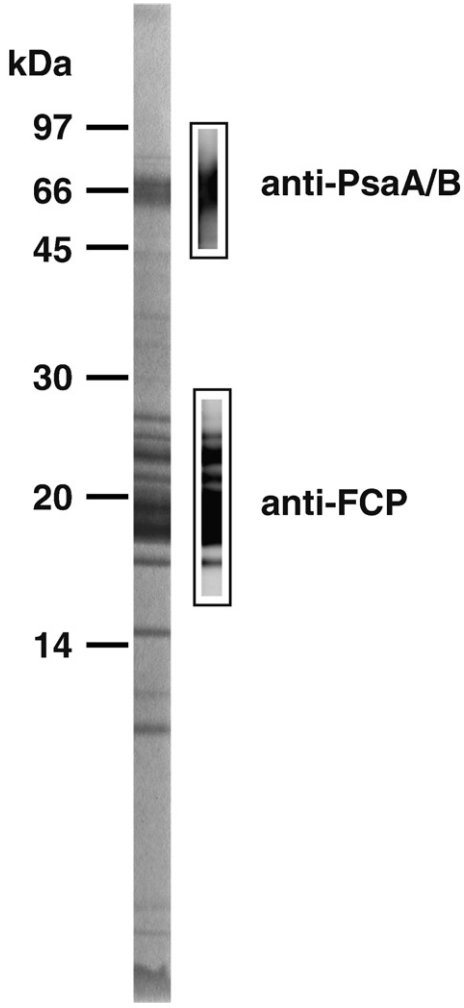

Fig. 3. Immunodetection of PsaA/B and FCP in the purified PS I complexes. The bands visualized by antibodies against PsaA/B or FCP are shown to the right of the corresponding bands stained by Coomassie Blue. Only the bands densely stained by anti-FCP are indicated as FCP in Fig. 1.

in [36]. Measurement of time-resolved fluorescence spectra (TRFS) was performed as described in [35] with some modifications. A Ti:sapphire laser (Mai Tai; Spectra-Physics in Newport Corporation, Irvine, CA) was used as the light source. The 460 nm pulse of 150 fs width was generated from the original 920 nm laser pulse operated at 80 MHz through a piece of BBO crystal. The laser pulse was passed through a 460 nm interference filter and focused onto the sample. The time resolution of the streak camera spectrophotometer for detection of the fluorescence signal was 5 ps [35]. The photoelectrons were collected in CCD images of 50,000 shots [35]. Global analysis of the fluorescence decay curve was conducted as described in [35].

3. Results

3.1. Isolation of thylakoid membranes

Highly photoactive thylakoid membranes were successfully isolated by simply disrupting diatom cells by freezing and thawing.

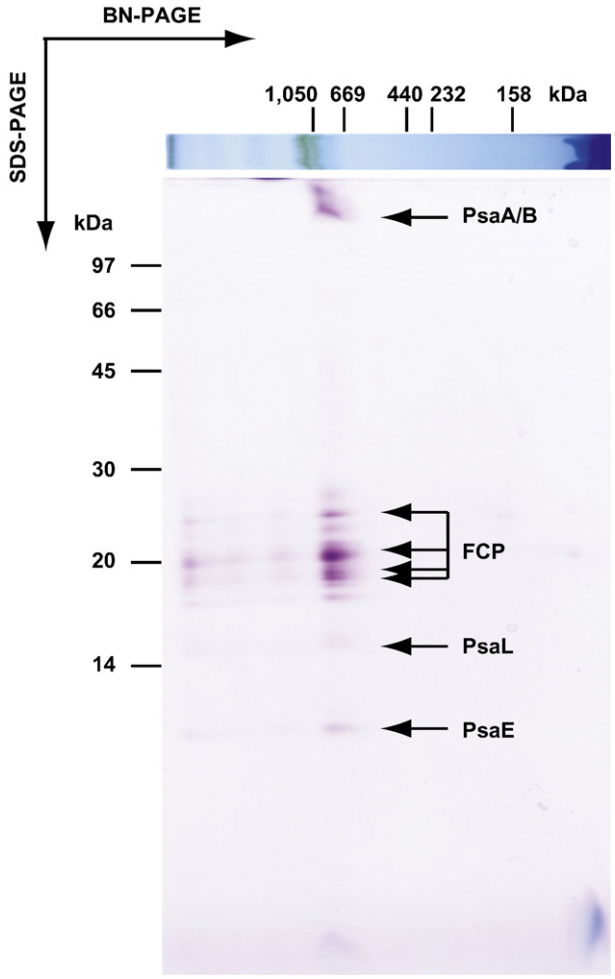

Fig. 4. Two-dimensional separation of purified PS I complexes from *Chaetoceros gracilis* using blue-native electrophoresis. PS I complexes equivalent to 6 μg Chl *a* were applied to BN-PAGE after incubation for 5 min with 0.05% DDM. The gel strip after BN-PAGE, which is shown at the top without staining, was developed on the second-dimensional SDS-PAGE. The second-dimensional picture was obtained after staining with Coomassie. Polypeptides separated from PS I complexes on the second-dimensional SDS-PAGE are indicated by arrows. The position of molecular-mass standards for the BN-PAGE were determined using a PS I trimer from *Synechocystis* 6803 (~1000 kDa), thyroglobulin (669 kDa), ferritin (440 kDa), catalase (232 kDa) and aldolase (158 kDa).

Table 2
Content of photosynthetic pigments in purified FCP–PS I super complexes

Pigments	Chl *c*1+*c*2	Fucoxanthin	DD+DT	Vx	β-carotene
Molar ratio per 224 Chl *a*	21.7 (±1.1)	54.7 (±3.3)	30.0 (±0.39)	0.72 (±0.087)	16.7 (±0.31)

Molar ratios of pigments per 224 Chl *a* are presented. Pigment quantities were determined by HPLC. The Chl *a* antenna size (224 Chl *a*) was assessed based on the concentration of photo-oxidizable P700. The values are expressed with ± SE (n=5).
Chl, chlorophyll; DD, diadinoxanthin; DT, diatoxanthin; Vx, violaxanthin.

The thylakoid membranes (Fig. 1, lane 1) showed oxygen-evolving activity of 230 μmol O_2 mg^{-1} Chl *a* h^{-1} with 0.5 mM 2,5-DCBQ as an electron acceptor. The activity was comparable to that of intact cells (Table 1). The most abundant protein in the isolated thylakoid membranes was FCP (Fig. 1, lane 1).

3.2. Purification of PS I complex

The thylakoid membranes solubilized with a detergent, DDM, also contained FCP as a main component (Fig. 1, lane 2). Following sucrose density gradient centrifugation of the

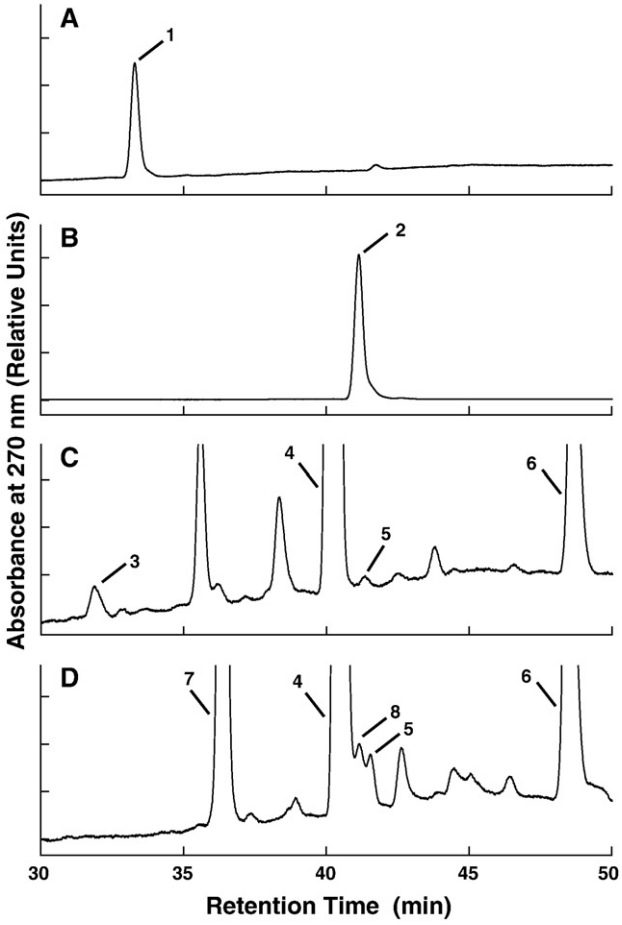

Fig. 5. HPLC traces of MK-4 (A), PhQ (B) and pigments extracted from diatom PS I complexes (C) and the spinach PS I fraction (D). Peak 1, MK-4; peak 2, PhQ; peak 3, MK-4; peak 4, Chl *a*; peak 5, Chl *a*'; peak 6, β-carotene; peak 7, Chl *b*; peak 8, PhQ. The Chl *a*/*b* ratio of the spinach PS I fraction was 7.8 (w/w), which confirmed its high enrichment of PS I.

solubilized membranes, most FCP and PS II complexes were separated as a brown band (Fig. 1, lane 3) in the ~0.4 M sucrose region (data not shown) and the PS I RC fraction formed a pellet (Fig. 1, lane 4). The purified PS I complex (Fig. 1, lane 5), which was obtained as a single peak by size-exclusion chromatography of the PS I-enriched pellet, had a molecular size of ~1000 kDa (Fig. 2). The purified PS I complex contained at least fourteen polypeptides between 3 and 70 kDa in size (Fig. 1, lane 5).

3.3. Polypeptide composition

The major bands at ~70 kDa were identified as PsaA and PsaB by immunoblotting using an antiserum specific to PsaA/B (Fig. 3). The four dark bands of ~18.5, 20.0 and 23.5 kDa were assigned to FCP proteins by immunoblotting using an antiserum raised against FCP (Fig. 3). All the distinct polypeptide bands other than those at ~20 kDa and PsaA/PsaB were subjected to N-terminal amino acid sequencing. A BLAST search [37] identified the ~15 kDa band with a N-terminal amino acid sequence of ANFIKPYNDDPFVG as PsaL. The ~10 kDa band with a N-terminal amino acid sequence of VSRGSKVRILRKExY (x represents an uncertain residue) was confirmed to be PsaE. N-terminal sequences of other polypeptides could not be determined. They were blocked. No polypeptides showed migration lengths identical to those of PS II components (data not shown).

The purified PS I complex, which was obtained after size-exclusion chromatography, contained FCP proteins as the major bands (Fig. 1, lane 5). The purified PS I complex was subjected to non-denaturing BN-PAGE and second-dimensional denaturing SDS-PAGE. Only a single green band was detected in the BN-PAGE (Fig. 4, top horizontal strip). The migration length of the purified PS I complex on BN-PAGE was comparable to that of the PS I trimer of *Synechocystis* 6803 (~1000 kDa) [23]. The second-dimensional SDS-PAGE of this single green band revealed thirteen distinct polypeptide spots including the FCP bands at ~20 kDa (Fig. 4), indicating the FCP proteins and the PS I RC complex were closely associated.

3.4. Pigment and quinone composition

The antenna size of the FCP–PS I super complex was estimated to be 224 (±4.0, $n=5$) Chl *a* per P700, which is in agreement with the value estimated for PS I isolated from *P. tricornutum* (225±25 per P700; [19]). HPLC analyses of the purified FCP–PS I super complex revealed an abundance of Chl *c* and xanthophylls such as fucoxanthin, DD, DT and violaxanthin (Vx) (Table 2).

PhQ, which is known to be the secondary electron acceptor A_1 in PS I, was eluted by reverse-phase HPLC between Chl *a* and Chl *a*' from the spinach PS I fraction (peak 8 in Figs. 5D and 6B). However, PhQ was not detected in the FCP–PS I super complex from *C. gracilis* (Fig. 5C). Instead, a quinone was detected at the retention time of 32–34 min (peak 3 in Fig. 5C) whose absorption spectrum was identical to that of MK-4 (Fig. 6A), which was eluted at the comparable retention time as peak 1 (Fig. 5A). The MK-4 detected in the *C. gracilis* FCP–PS I super complex was estimated to have a molecular ratio of 1.59 (±0.10, $n=5$) per P700.

3.5. Absorption spectrum of purified FCP–PS I super complex

The absorbance between 450 and 550 nm in the spectrum of the purified FCP–PS I super complex is smaller than those in the spectra of thylakoid membranes and FCP, indicating that the purified FCP–PS I super complex contained lower amounts of

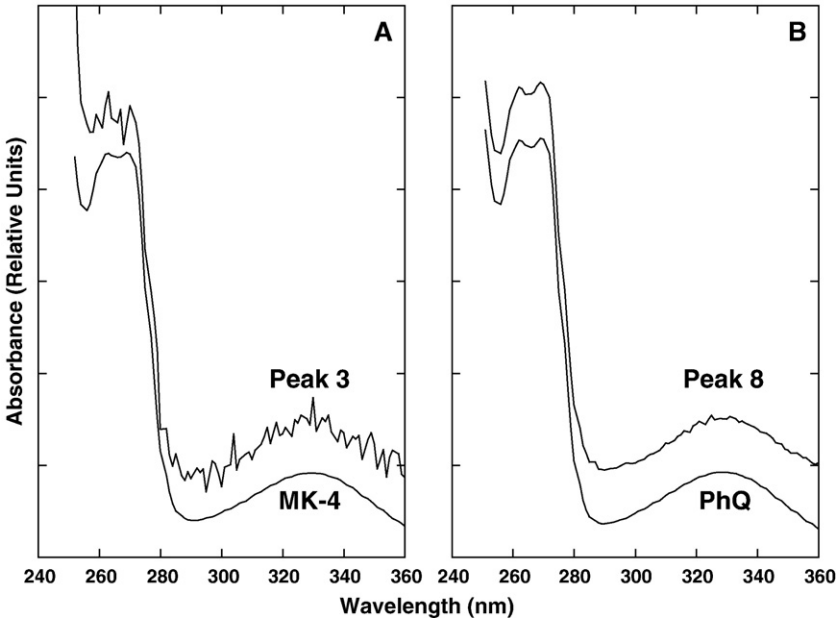

Fig. 6. Absorption spectra of MK-4 and PhQ compared to those of peak 3 (A) and peak 8 (B) in Fig. 5, respectively. The spectra amplitudes were adjusted to the same level at 270 nm. The spectrum for peak 8 of the spinach PS I fraction was obtained using extracted pigments whose Chls had been converted to pheophytins by addition of 0.005 N HCl to eliminate interference by Chls *a* and *a*'.

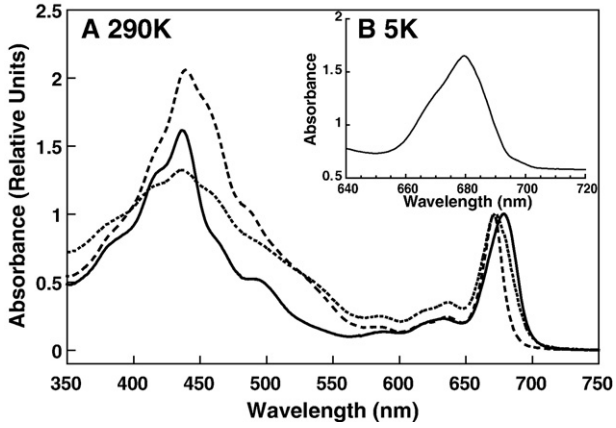

Fig. 7. Absorption spectra of the FCP fraction, thylakoid membranes and purified FCP–PS I super complexes of *Chaetoceros gracilis*. A, absorption spectra measured at 290 K. Dotted line, thylakoid membranes; dashed line, FCP fraction; and solid line, purified FCP–PS I super complexes. The Chl *a* concentration was 5 μg mL^{-1}. Absorption spectra were measured at room temperature and normalized at the red peak. B, Absorption spectrum of the FCP–PS I super complex (7.5 μg Chl *a* mL^{-1}) measured at 5 K.

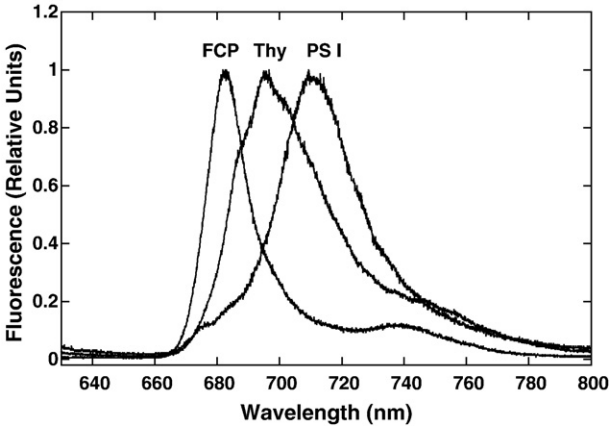

Fig. 8. Steady-state fluorescence emission spectra at 77 K. FCP, FCP fraction; Thy, thylakoid membranes; PS I, purified FCP–PS I super complexes from *Chaetoceros gracilis*. The Chl *a* concentration was 0.8 mg mL^{-1}.

Chl *c* and carotenoids with respect to Chl *a*. The purified FCP–PS I super complex gave a red peak at 679 nm, which is a remarkably longer wavelength than those of the thylakoid membranes (675 nm) and FCP (671 nm). The band width at the half maximum in the FCP–PS I super complex is comparable to that of thylakoid membranes, but is wider than that of FCP. Neither the thylakoid membranes nor the purified FCP–PS I super complexes contained components absorbing at ~705 nm corresponding to the so-called red Chls, which are found in most PS I RCs [38]. The absorption spectrum at 5 K of the purified FCP–PS I super complex (Fig. 7B) showed almost no absorption at ~705 nm, which confirmed the absence of red Chls. The spectrum showed an asymmetric peak at 680 nm, extended on the shorter wavelength side, which indicated the presence of FCP.

3.6. Energy transfer

The steady-state fluorescence emission spectrum at 77 K of thylakoid membranes showed a distinct peak at 696 nm and shoulder peaks at ~685 nm and 710 nm (Fig. 8, Thy). The FCP fraction emitted peak fluorescence at a shorter wavelength of 683 nm (Fig. 8, FCP). The purified FCP–PS I super complex emitted peak fluorescence at 710 nm (Fig. 8, PS I), and produced very low fluorescence of FCP at 680 ~ 690 nm despite the high content of FCP (Fig. 1, lane 5 and Table 2), which is suggestive of efficient energy transfer from FCP to the PS I RC complex.

To address energy transfer from FCP to the PS I core, the fluorescence decay kinetics and time-resolved fluorescence spectrum (TRFS) [35] of the purified FCP–PS I super complex were obtained (Fig. 9). The three-dimensional image (Fig. 9B) demonstrated the gradual transition of the fluorescence peak from 690 nm to longer wavelengths. The kinetics at 679 nm (Fig. 9A, line a) calculated from the image showed very rapid decay within 100 ps, while those at 697 and 714 nm (Fig. 9A, lines b and c, respectively) showed slow rises with much slower decays, which was indicative of energy transfer from the short- to long-wavelength fluorescence bands.

To clarify the complete TRFS picture, a global multi-exponential analysis of the decay kinetics was performed; the resulting decay-associated spectra (DAS) [35] are shown in Fig. 10. When the PS I complex was excited at 460 nm, four DAS components were obtained with time constants of 16, 57, 246 and larger than 3000 ps, respectively. Positive peaks were located at around 685, 695, 710 and 715 nm. A similar result was obtained when the complex was excited at 440 nm (data not shown). The fastest 16 ps DAS component showed a positive peak at ~685 nm. The following three DAS components had time constants of 57 ps, 246 ps and longer than 3 ns with positive peaks but lower amplitudes at ~695, ~710 and

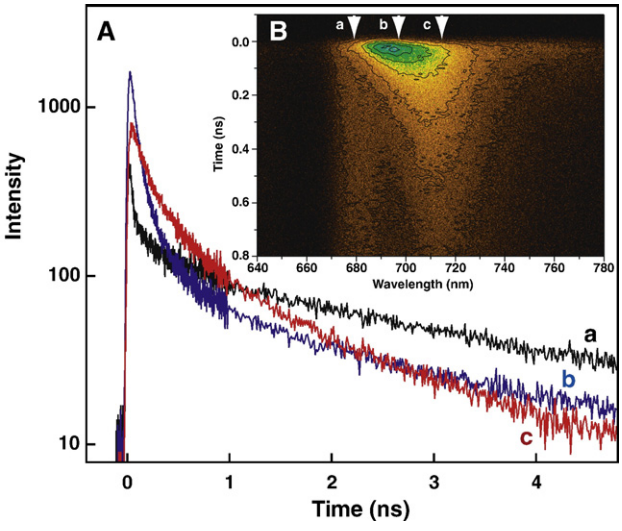

Fig. 9. Decay time course and wavelength-decay time image of fluorescence at 77 K for the *Chaetoceros gracilis* FCP–PS I super complex. Fluorescence decay time courses at different wavelengths were calculated from the measurements at 77 K as shown in B. The symbols a, b and c correspond to 679, 697, and 714 nm, respectively. B, fluorescence emission excited by the repetitive 150 fs, 460 nm laser light was measured with the streak camera system. The emission spectrum is painted from cold to warm colors to represent the increase in fluorescence intensity. The Chl *a* concentration was 0.15 mg mL^{-1}.

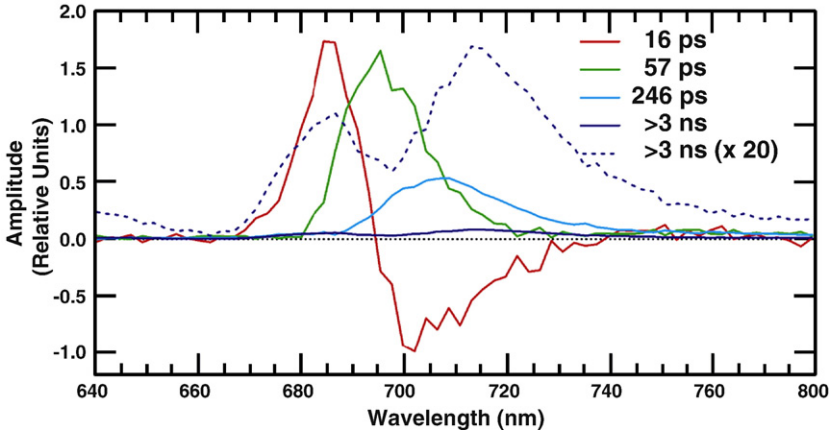

Fig. 10. Decay-associated spectra (DAS) obtained through the global multi-exponential analysis of the fluorescence decay kinetics shown in Fig. 9. Each fluorescence spectrum belongs to the decay component whose time constant is 16–24 ps (red line, 16 ps), 45–57 ps (green line, 57 ps), 236–336 ps (blue line, 246 ps) and larger than 3 ns (dark blue line, >3 ns), respectively. The spectrum of the fluorescence component whose decay time constant is larger than 3 ns is shown at a ×20 scale (dashed dark blue line, >3 ns).

~715 nm, respectively. These results demonstrate that excitation energy sequentially transferred from the fastest DAS component (F685) to the slower DAS components (F695, F710 and F715 in Fig. 11). The peak wavelength of the fastest DAS component was identical to that observed in the FCP fraction shown in Fig. 8. Fluorescence from FCP could not be clearly recognized in other slower DAS components (Fig. 10). It seems that the fluorescence from the energy transfer-active fraction of FCP mainly contributes to the fastest DAS component (see below). Therefore, the features of the fastest DAS component, together with those of the other DAS components, seem to represent excitation energy transfer from FCP to PS I RC. A small contribution of fluorescence at ~685 nm in the slowest DAS component (>3 ns) might correspond to the small fraction of FCP that could not transfer excitation energy to PS I RC in the purified complexes.

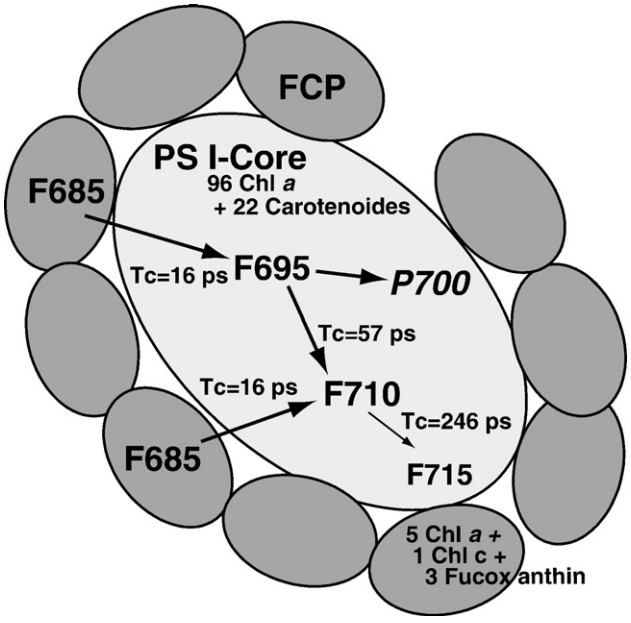

Fig. 11. Model of the FCP–PS I super complex and light energy transfer within the complex. Tc, time constant.

4. Discussion

4.1. Isolation of photoactive thylakoid membranes

Thylakoid membranes were isolated from *C. gracilis* by a very simple process, which consisted of disruption of cells by freezing and thawing followed by centrifugation. The integrity of the thylakoid membranes is demonstrated by the high oxygen-evolving activity (as high as 230 μmol O_2 mg^{-1} Chl h^{-1}), which is comparable to that of intact cells. The activity is significantly higher than the rate of 52 μmol O_2 mg^{-1} Chl h^{-1} reported by Martinson et al. [20]. The method was also used to prepare highly active membranes from *T. pseudonana*, indicating that it is applicable for the biochemical study of other diatoms.

4.2. Composition of polypeptides in the purified FCP–PS I super complex

The polypeptide profile of the purified FCP–PS I super complex (Fig. 1, lane 5) analyzed by a specialized gel system [27,39] indicated the presence of PsaA, PsaB, PsaE and PsaL (Fig. 1). PsaE and PsaL were identified for the first time in a purified diatom PS I preparation. Recently, PsaL was detected in a mixed PS I/PS II fraction from *P. tricornutum* by mass spectrometry analysis [40]. At least six more polypeptides (12 polypeptides in total) were detected in the present study, although their identification awaits internal amino acid sequencing. The PS I composition of *C. gracilis* is somewhat different from that of the PS I preparation from a pennate diatom, *P. tricornutum* [19], which contained at least six additional polypeptides of 30–50 kDa. The PS I fraction associated with FCP obtained from a centric diatom, *C. cryptica*, also showed additional polypeptides of ~30 kDa [21]. Since the crystallized PS I RC complex of cyanobacteria [23] and higher plants, which retains LHC [22,41], did not contain polypeptides in this molecular size range, the PS I complex

obtained in the present study seems to be highly purified. Purification of a FCP–PS I complex from *P. tricornutum* has recently been reported [42], after the preparation of the present report. However, our method yielded a more highly purified polypeptide profile for *C. gracilis* than those for *P. tricornutum* [42] and *C. cryptica* [21]. A remarkable feature of our purified PS I complex is seen in its association with multiple specific FCP proteins, as demonstrated by their co-migration with the PS I RC complex throughout BN-PAGE (Fig. 4). FCP proteins may exist at the periphery of the PS I RC complex in the form of higher oligomers [43] (see Fig. 11). The integrity of the purified FCP–PSI complex we obtained was indicated by the low contribution of FCP to the fluorescence emission spectrum (Fig. 8), despite the high FCP content (lane 5 in Fig. 1 and Table 2). This result contrasted with those for the FCP–PS I complexes from *C. cryptica* [21] and *P. tricornutum* [42], which showed high FCP fluorescence. In *C. cryptica*, the apparent uncoupling of the FCP and PS I RC complex might be due to the over-solubilization of thylakoid membranes from using a DDM concentration as high as 10% (w/w), since green bands were reported after sucrose density centrifugation or deriphat-PAGE [21]. Greenish bands were also obtained following sucrose density gradient centrifugation in the initial stages of our study, but subsequently we optimized the amount of DDM until only brown bands were obtained. As well, the use of a French pressure cell to disrupt the cell [42,44] might have affected the integrity of the FCP–PS I complex in *P. tricornutum*.

4.3. Characteristics of the FCP–PS I super complex

The number of FCP proteins bound to the PS I RC complex can be estimated as follows. The size of the monomeric cyanobacterial PS I RC complex is 356 kDa based on the inclusion of 96 Chl *a* and 22 carotenoid molecules [23]. The extra pigments in our purified PS I complex comprise 128 Chl *a*, 22 Chl *c* and 80 carotenoid molecules (Table 2), which altogether correspond to ~170 kDa. The molecular size of the purified PS I complex was estimated to be ~1000 kDa (Figs. 2 and 4). The remaining unassigned mass (~470 kDa) is attributed to FCP apoproteins. Since the molecular size of FCP apoproteins could be assumed to be ~19 kDa (Fig. 1), the number of FCPs was estimated to be ~25 copies per PS I, which is quite large compared to that of LHC bound to pea PS I RC complex [22,41]. If we assume that the extra pigments are evenly distributed with each FCP protein, the number of Chl *a*, Chl *c* and fucoxanthin molecules on each FCP would be about 5, 1 and 3, respectively (Chl *a*:Chl *c*:fucoxanthin = 100:17.2:42.7). The exact stoichiometry of pigments on a single FCP protein has not been reported yet.

The estimated pigment stoichiometry is comparable to that reported for the native LHCF-I fraction obtained from a brown alga (Chl *a*:Chl *c*:fucoxanthin = 100:19.3:58.1) [45] but differs somewhat from that obtained for the isolated FCP in the present study (Chl *a*:Chl *c*:fucoxanthin = 100:44.9:130). The latter is similar to that reported for 'native' LH from *P. tricornutum* (Chl *a*:Chl *c*:fucoxanthin = 100:38:127) [19]. However, the molar pigment ratios from different FCP preparations vary considerably (e.g., [14,42,45,47,48]), and may reflect different peptide compositions from the expressions of the many FCP genes known to come from diatoms [5,46]. Similarly, the relatively high ratio of Chl *a* to Chl *c* and fucoxanthin reported here for the purified FCP–PS I super complex may reflect the involvement of PS I-specific FCP genes.

4.4. Menaquinone as the secondary electron acceptor A_1

MK-4 was detected at a ratio of 1.59 molecules per P700 in the purified PSI complex instead of phylloquinone, which is known to function as the secondary electron acceptor A_1 or its counterpart $A_1^{'}$. A portion of MK-4 might be released during the purification process. The role of phylloquinone as A_1 or its counterpart $A_1^{'}$. is known to be functionally substituted by artificial quinones [49–51]. However, until now only two species, a primitive cyanobacterium, *Gloeobacter violaceus* [52], and a primitive red alga, *Cyanidium caldarium* [53], have been reported to use MK-4 as A_1. The PS I complexes isolated from a centric diatom, *T. pseudonana*, and a pennate diatom, *P. tricornutum*, also use MK-4 rather than phylloquinone (Ikeda et al., unpublished data). These results indicate that diatoms may be phylogenetically unique with regard to A_1.

4.5. Excitation energy transfer within the FCP–PSI super complex

Published reports of the fluorescence peak of FCPs varies from ~675 to ~686 nm [19,54,55]. The peak wavelength of the FCP fraction obtained in the present study was ~685 nm, which was identical to that of the fastest DAS component. Together with the biochemical characteristics of the FCP–PS I super complex obtained, the identity of the fastest DAS component (F685) can be concluded to be FCP. The excitation energy seems to be transferred from FCP to the chromophores (F695) in the PS I RC complex with a time constant of 16 ps, with subsequent sequential energy migration to P700 or other fluorescent components. Direct energy transfer from FCPs to the PS I RC complex was demonstrated for the first time in the present study. Trautman et al. reported that the excitation energy transfer from fucoxanthin to Chl occurred in the range of 0.2 ps in *P. tricornutum* cells at room temperature [56]. More recently, Papagiannakis et al. isolated FCP from *Cyclotella meneghiniana* and demonstrated that excitation energy transfer occurred on a time scale of 100 fs from Chl *c* to Chl *a*, and that rapid energy transfer from fucoxanthin and Chl *c* to Chl *a* occurred at room temperature [48]. Therefore, we can hypothesize that excitation energy trapped by accessory pigments (fucoxanthin and Chl *c*) of FCP migrates to Chl *a* at the sub-picosecond time scale, and then to Chl *a* on the PS I RC complex on a time scale of tens of picoseconds. The tightly-bound FCPs in PS I may also mediate energy transfer between the weakly bound peripheral FCPs and the PS I RC complex.

4.6. Chlorophylls on the core complex

The fluorescence spectrum of the isolated diatom thylakoids was quite different from that observed in thylakoid membranes or cells of green plants and cyanobacteria, in which the long-wavelength fluorescence (720–740 nm) peaks have been

attributed to PS I and the shorter wavelength peaks at 680–690 nm to PS II (as reviewed in [57]). It is difficult to assign PS I fluorescence in the fluorescence spectrum of the thylakoid membranes of *C. gracilis* (Fig. 8). The steady-state fluorescence peak for the purified FCP–PS I super complex was 710 nm at 77 K, which is 10–30 nm shorter than that for PS I of many other organisms. Similarly blue-shifted PS I fluorescence has been reported for several species [58–62].

It is evident that the amount of the PS I complex component that absorbs light at ~705 nm (red Chls) is small in diatoms (Fig. 7). In cyanobacterial PS I RC complexes, nine to twelve Chls are assumed to be red Chls associated with PsaA, PsaB and PsaL [23]. In *G. violaceus*, which lacks long-wavelength fluorescence emitters [60,63], the comparison of deduced amino acid sequences from a wide variety of organisms (data not shown) suggested that the loop PsaB, where Chls B31, B32, and B33 were coordinated [23,38], was modified so that red Chls were absent. However, in diatoms, the deduced amino acid sequences of PsaB did not show similar modifications to those in *G. violaceus*. Further analysis of the structural basis for the absence of red Chls must await a high-resolution structure of a PS I complex deficient in red Chls from Chl *c*-containing algae.

The light intensity in the habitat of marine diatoms may be low and, furthermore, the light quality is totally blue-shifted [7]. *C. gracilis*, therefore, might not retain red Chls that are not useful in such environments. Alternatively, the DD cycle within the FCP might take their place to dissipate the excess light energy on PS I [15,64]. Therefore, the tight binding and efficient energy transfer between FCP and the PS I core seems to be essential for the efficient function of diatom PS I.

4.7. Concluding remarks

In this study the diatom PS I complex was highly purified as a super complex with multiple FCP molecules (Fig. 11). High amounts of FCPs that bind fucoxanthin and transfer excitation energy efficiently to PS I will contribute to the light-harvesting function of PSI, especially in the blue-shifted light environment in the oceans. The gentle method of purifying thylakoids and the FCP–PS I super complex developed in this study will be useful for future studies of photosynthetic mechanisms and the metabolic systems of diatoms, as well as contributing to a better understanding of the global carbon cycle.

Acknowledgments

We are grateful to Drs. Beverly R. Green and Isao Enami for providing antibodies and Dr. Sadao Wakabayashi for his technical assistance with N-terminal amino acid sequencing. We also thank two anonymous referees and the journal editor for their constructive comments that improved our final manuscript. This work was supported by the Ministry of Education, Culture, Sports, Science and Technology, Japan (18054028 to YK and 17370055 to SI) and grants from Hyogo Prefecture (YK), the National Institute of Polar Research (16–28, YK) and the 21st Century Center of Excellence Program (COE) from the Ministry of Education, Culture, Sports, Science and Technology, Japan (KS, SI).

References

[1] P. Falkowski, R.J. Scholes, E. Boyle, J. Canadell, D. Canfield, J. Elser, N. Gruber, K. Hibbard, P. Högberg, S. Linder, F.T. Mackenzie, B. Moor III, T. Pedersen, Y. Rosenthal, S. Seitzinger, V. Smetacek, W. Steffen, The global carbon cycle: a test of our knowledge of earth as a system, Science 290 (2000) 291–296.

[2] D.M. Nelson, P. Tréguer, M.A. Brzezinski, A. Leynaert, B. Quéguiner, Production and dissolution of biogenic silica in the ocean: revised global estimates, comparison with regional data and relationship to biogenic silica sedimentation, Global Biogeochem. Cycles 9 (1995) 359–372.

[3] C.B. Field, M.J. Behrenfeld, J.T. Randerson, P. Falkowski, Primary production of the biosphere: integrating terrestrial and oceanic components, Science 281 (1998) 237–240.

[4] R.F. Strzepek, P.J. Harrison, Photosynthetic architecture differs in coastal and oceanic diatoms, Nature 431 (2004) 689–692.

[5] E.V. Armbrust, J.A. Berges, C. Bowler, B.R. Green, D. Martinez, N.H. Putnam, S. Zhou, A.E. Allen, K.E. Apt, M. Bechner, M.A. Brzezinski, B.K. Chaal, A. Chiovitti, A.K. Davis, M.S. Demarest, J.C. Detter, T. Glavina, D. Goodstein, M.Z. Hadi, U. Hellsten, M. Hildebrand, B.D. Jenkins, J. Jurka, V.V. Kapitonov, N. Kröger, W.W. Lau, T.W. Lane, F.W. Larimer, J.C. Lippmeier, S. Lucas, M. Medina, A. Montsant, M. Obornik, M.S. Parker, B. Palenik, G.J. Pazour, P.M. Richardson, T.A. Rynearson, M.A. Saito, D.C. Schwartz, K. Thamatrakoln, K. Valentin, A. Vardi, F.P. Wilkerson, D.S. Rokhsar, The genome of the diatom *Thalassiosira pseudonana*: ecology, evolution, and metabolism, Science 306 (2004) 79–86.

[6] M.P. Oudot-Le Secq, J. Grimwood, H. Shapiro, E.V. Armbrust, C. Bowler, B.R. Green, Chloroplast genomes of the diatoms *Phaeodactylum tricornutum* and *Thalassiosira pseudonana*: comparison with other plastid genomes of the red lineage, Mol. Genet. Genomics 277 (2007) 427–439.

[7] P.G. Falkowski, J.A. Raven, Aquatic Photosynthesis, Princeton Univ Press, Princeton, NJ, 2007.

[8] A. Melis, Regulation of photosystem stoichiometry in oxygenic photosynthesis, in: S. Miyachi, R. Kanai, S. Katoh (Eds.), Regulation of Photosynthetic Processes, The Botanical Society of Japan, Tokyo, 1991, pp. 9–28.

[9] B.M. Smith, A. Melis, Photochemical apparatus organization in the diatom *Cylindrotheca fusiformis*: photosystem stoichiometry and excitation distribution in cells grown under high and low irradiance, Plant Cell Physiol. 29 (1988) 761–769.

[10] P.G. Falkowski, T.G. Owens, A.C. Ley, D.C. Mauzerall, Effects of growth irradiance levels on the ratio of reaction centers in two species of marine phytoplankton, Plant Physiol. 68 (1981) 969–973.

[11] J.A. Raven, M.C.W. Evans, R.E. Korb, The role of trace metals in photosynthetic electron transport in O_2-evolving organisms, Photosynth. Res. 60 (1999) 111–150.

[12] P.G. Falkowski, T.G. Owens, Light–shade adaptation: tow strategies in marine phytoplankton, Plant Physiol. 66 (1980) 592–595.

[13] A. Ban, S. Aikawa, H. Hattori, H. Sasaki, M. Sampei, S. Kudoh, M. Fukuchi, K. Satoh, Y. Kashino, Comparative analysis of photosynthetic properties in ice algae and phytoplankton inhabiting Franklin Bay, the Canadian Arctic, with those in mesophilic diatoms during CASES 03–04, Polar Biosci. 19 (2006) 11–28.

[14] G. Guglielmi, J. Lavaud, B. Rousseau, A.L. Etienne, J. Houmard, A.V. Ruban, The light-harvesting antenna of the diatom *Phaeodactylum tricornutum*. Evidence for a diadinoxanthin-binding subcomplex, FEBS J. 272 (2005) 4339–4348.

[15] B. Demmig-Adams, Carotenoids and photoprotection in plants: a role for the xanthophyll zeaxanthin, Biochim. Biophys. Acta 1020 (1990) 1–24.

[16] M. Olaizola, H.Y. Yamamoto, Short-term response of the diadinoxanthin cycle and fluorescence yield to high irradiance in *Chaetoceros muelleri* (Bacillariophyceae), J. Phycol. 30 (1994) 606–612.

[17] W. Arsalane, B. Rousseau, J.-C. Duval, Influence of the pool size of the xanthophyll cycle on the effects of light stress in a diatom: competition between photoprotection and photoinhibition, Photochem. Photobiol. 60 (1994) 237–243.

[18] Y. Kashino, S. Kudoh, Concerted response of xanthophyll-cycle pigments in a marine diatom, *Chaetoceros gracilis*, to the sifts of light condition, Phycol. Res. 51 (2003) 168–172.

[19] C. Berkaloff, L. Caron, B. Rousseau, Subunit organization of PSI particles from brown algae and diatoms: polypeptide and pigment analysis, Photosynth. Res. 23 (1990) 181–193.
[20] T.A. Martinson, M. Ikeuchi, F.G. Plumley, Oxygen-evolving diatom thylakoid membranes, Biochim. Biophys. Acta 1409 (1998) 72–86.
[21] T. Brakemann, W. Schlörmann, J. Marquardt, M. Nolte, E. Rhiel, Association of fucoxanthin chlorophyll *a/c*-binding polypeptides with photosystems and phosphorylation in the centric diatom *Cyclotella cryptica*, Protist 157 (2006) 463–475.
[22] A. Ben-Shem, F. Frolow, N. Nelson, Crystal structure of plant photosystem I, Nature 426 (2003) 630–635.
[23] P. Jordan, P. Fromme, H.T. Witt, O. Klukas, W. Saenger, N. Krauß, Three-dimensional structure of cyanobacterial photosystem I at 2.5 Å resolution, Nature 411 (2001) 909–917.
[24] R.R. Guillard, J.H. Ryther, Studies of marine planktonic diatoms. I. *Cyclotella nana* Hustedt, and *Detonula confervacea* (cleve) Gran, Can. J. Microbiol. 8 (1962) 229–239.
[25] Y. Kashino, W.M. Lauber, J.A. Carroll, Q. Wang, J. Whitmarsh, K. Satoh, H.B. Pakrasi, Proteomic analysis of a highly active photosystem II preparation from the cyanobacterium *Synechocystis* sp. PCC 6803 reveals the presence of novel polypeptides, Biochemistry 41 (2002) 8004–8012.
[26] Y. Kashino, H. Koike, K. Satoh, Isolation of oxygen-evolving photosystem II particles with the intact Q_B site, in: N. Murata (Ed.), Research in Photosynthesis, vol. II, Kluwer, 1992, pp. 163–166.
[27] Y. Kashino, H. Koike, K. Satoh, An improved sodium dodecyl sulfate-polyacrylamide gel electrophoresis system for the analysis of membrane protein complexes, Electrophoresis 22 (2001) 1004–1007.
[28] Y. Kashino, I. Enami, K. Satoh, S. Katoh, Immunological cross-reactivity among corresponding proteins of photosystems I and II from widely divergent photosynthetic organisms, Plant Cell Physiol. 31 (1990) 479–488.
[29] H. Schägger, Blue native electrophoresis, in: C. Hunte, G. von Jagow, H. Schägger (Eds.), Membrane Protein Purification and Crystallization: A Practical Guide, Academic Press, Amsterdam, 2002, pp. 105–130.
[30] K. Furuya, M. Hayashi, Y. Yabushita, HPLC determination of phytoplankton pigments using *N,N*-dimethylformamide, J. Oceanogr. 54 (1998) 199–203.
[31] P.J. Dunphy, A.F. Brodie, The structure and function of quinones in respiratory metabolism, in: D.B. McCormick, L.D. Wright (Eds.), Vitamins and Coenzymes, Part C, Methods in Enzymology, vol. 18, Academic Press, New York, 1971, pp. 407–461.
[32] T. Hiyama, B. Ke, Difference spectra and extinction coefficients of P700, Biochim. Biophys. Acta 267 (1972) 160–171.
[33] S.W. Jeffrey, G.F. Humphrey, New spectroscopic equations for determining chlorophylls *a*, *b*, *c*1 and *c*2 in higher plants, algae and natural phytoplankton, Biochem. Physiol. Pflanzen 167 (1975) 191–194.
[34] R.J. Porra, W.A. Thompson, P.E. Kriedemann, Determination of accurate extinction coefficients and simultaneous equations for assaying chlorophylls *a* and *b* extracted with four different solvents: verification of the concentration of chlorophyll standards by atomic absorption spectroscopy, Biochim. Biophys. Acta 975 (1989) 384–394.
[35] M. Komura, Y. Shibata, S. Itoh, A new fluorescence band F689 in photosystem II revealed by picosecond analysis at 4–77 K: function of two terminal energy sinks F689 and F695 in PS II, Biochim. Biophys. Acta 1757 (2006) 1657–1668.
[36] N. Inoue-Kashino, Y. Kashino, K. Satoh, I. Terashima, H.B. Pakrasi, PsbU provides a stable architecture for the oxygen-evolving system in cyanobacterial photosystem II, Biochemistry 44 (2005) 12214–12228.
[37] S.F. Altschul, T.L. Madden, A.A. Schäffer, J. Zhang, Z. Zhang, W. Miller, D.J. Lipman, Gapped BLAST and PSI-BLAST: a new generation of protein database search programs, Nucleic Acids Res. 25 (1997) 3389–3402.
[38] M. Byrdin, P. Jordan, N. Krauss, P. Fromme, D. Stehlik, E. Schlodder, Light harvesting in photosystem I: modeling based on the 2.5-Å structure of photosystem I from *Synechococcus elongatus*, Biophys. J. 83 (2002) 433–457.
[39] Y. Kashino, Separation methods in the analysis of protein membrane complexes, J. Chromatogr. B 797 (2003) 191–216.
[40] B. Lepetit, D. Volke, M. Szabo, R. Hoffmann, G. Garab, C. Wilhelm, R. Goss, Spectroscopic and molecular characterization of the oligomeric antenna of the diatom *Phaeodactylum tricornutum*, Biochemistry 46 (2007) 9813–9822.
[41] A. Amunts, O. Drory, N. Nelson, The structure of a plant photosystem I supercomplex at 3.4 Å resolution, Nature 447 (2007) 58–63.
[42] T. Veith, C. Büchel, The monomeric photosystem I-complex of the diatom *Phaeodactylum tricornutum* binds specific fucoxanthin chlorophyll proteins (FCPs) as light-harvesting complexes, Biochim. Biophys. Acta 1767 (2007) 1428–1435.
[43] C. Büchel, Fucoxanthin-chlorophyll proteins in diatoms: 18 and 19 kDa subunits assemble into different oligomeric states, Biochemistry 42 (2003) 13027–13034.
[44] L.A. Gugliemelli, H.J. Dutton, P.A. Jursinic, H.W. Siegelman, Energy transfer in a light-harvesting carotenoid-chlorophyll *c*-chlorophyll *a*-protein of *Phaeodactylum tricornutum*, Photochem. Photobiol. 33 (1981) 903–907.
[45] A. De Martino, D. Douady, M. Quinet-Szely, B. Rousseau, F. Crepineau, K. Apt, L. Caron, The light-harvesting antenna of brown algae: highly homologous proteins encoded by a multigene family, Eur. J. Biochem. 267 (2000) 5540–5549.
[46] S. Scala, N. Carels, A. Falciatore, M.L. Chiusano, C. Bowler, Genome properties of the diatom *Phaeodactylum tricornutum*, Plant Physiol. 129 (2002) 993–1002.
[47] A. Beer, K. Gundermann, J. Beckmann, C. Büchel, Subunit composition and pigmentation of fucoxanthin-chlorophyll proteins in diatoms: evidence for a subunit involved in diadinoxanthin and diatoxanthin binding, Biochemistry 45 (2006) 13046–13053.
[48] E. Papagiannakis, I.H.M. van Stokkum, H. Fey, C. Büchel, R. van Grondelle, Spectroscopic characterization of the excitation energy transfer in the fucoxanthin-chlorophyll protein of diatoms, Photosynth. Res. 86 (2005) 241–250.
[49] I. Ikegami, S. Itoh, M. Iwaki, Selective extraction of antenna chlorophylls, carotenoids and quinones from photosystem I reaction center, Plant Cell Physiol. 41 (2000) 1085–1095.
[50] M. Iwaki, S. Itoh, Electron transfer in spinach photosystem I reaction center containing benzo-, naphtho- and anthraquinones in place of phylloquinone, FEBS Lett. 256 (1989) 11–16.
[51] T.W. Johnson, B. Zybailov, A.D. Jones, R. Bittl, S. Zech, D. Stehlik, J.H. Golbeck, P.R. Chitnis, Recruitment of a foreign quinone into the A1 site of photosystem I. In vivo replacement of plastoquinone-9 by media-supplemented naphthoquinones in phylloquinone biosynthetic pathway mutants of *Synechocystis* sp. PCC 6803, J. Biol. Chem. 276 (2001) 39512–39521.
[52] M. Mimuro, T. Tsuchiya, H. Inoue, Y. Sakuragi, Y. Itoh, T. Gotoh, H. Miyashita, D.A. Bryant, M. Kobayashi, The secondary electron acceptor of photosystem I in *Gloeobacter violaceus* PCC 7421 is menaquinone-4 that is synthesized by a unique but unknown pathway, FEBS Lett. 579 (2005) 3493–3496.
[53] E. Yoshida, A. Nakamura, T. Watanabe, Reversed-phase HPLC determination of chlorophyll *a′* and naphthoquinones in photosystem I of red algae: existence of two menaquinone-4 molecules in photosystem I of *Cyanidium caldarium*, Anal. Sci. 19 (2003) 1001–1005.
[54] J. Lavaud, B. Rousseau, A.L. Etienne, Enrichment of the light-harvesting complex in diadinoxanthin and implications for the nonphotochemical fluorescence quenching in diatoms, Biochemistry 42 (2003) 5802–5808.
[55] T.G. Owens, E.R. Wold, Light-harvesting function in the diatom *Phaeodactylum tricornutum*: I. Isolation and characterization of pigment–protein complexes, Plant Physiol. 80 (1986) 732–738.
[56] J.K. Trautman, A.P. Shreve, T.G. Owens, A.C. Albrecht, Femtosecond dynamics of carotenoid to chlorophyll energy transfer in thylakoid membrane preparations from *Phaeodactylum tricornutum* and *Nannochloropsis* sp, in: M. Baltscheffsky (Ed.), Recent Progress of Photosynthesis Research, vol. II, Kluwer Academic Publishers, Dordrecht, 1990, pp. 289–292.
[57] S. Itoh, K. Sugiura, in: G.C. Papageorgiou (Ed.), Chlorophyll *a* Fluorescence: A Signature of Photosynthesis, vol. 19, Springer, Dordrech, The Netherlands, 2004, pp. 231–250.
[58] S. Lin, R.S. Knox, Studies of excitation energy transfer within the green alga *Chlamydomonas reinhardtii* and its mutants at 77 K, Photosynth. Res. 27 (1991) 157–168.
[59] D. Mangels, J. Kruip, S. Berry, M. Rögner, E.J. Boekema, F. Koenig, Photosystem I from the unusual cyanobacterium *Gloeobacter violaceus*, Photosynth. Res. 72 (2002) 307–319.

[60] M. Mimuro, T. Ookubo, D. Takahashi, T. Sakawa, S. Akimoto, I. Yamazaki, H. Miyashita, Unique fluorescence properties of a cyanobacterium *Gloeobacter violaceus* PCC 7421: reasons for absence of the long-wavelength PSI Chl *a* fluorescence at −196 °C, Plant Cell Physiol. 43 (2002) 587–594.
[61] K. Satoh, D.C. Fork, Chlorophyll fluorescence transients as indications of changes in the redox state of plastoquinone in intact *Bryopsis corticulans*, Plant Sci. Lett. 29 (1983) 133–144.
[62] K. Sugahara, N. Murata, A. Takamiya, Fluorescence of chlorophyll in brown algae and diatoms, Plant Cell Physiol. 12 (1971) 377–385.
[63] F. Koenig, M. Schmidt, *Gloeobacter violaceus* — investigation of an unusual photosynthetic apparatus. Absence of the long wavelength emission of photosystem I in 77 K fluorescence spectra, Physiol. Plant. 94 (1995) 621–628.
[64] A. Wehner, S. Storf, P. Jahns, V.H. Schmid, De-epoxidation of violaxanthin in light-harvesting complex I proteins, J. Biol. Chem. 279 (2004) 26823–26829.